



Realization of a single-beam mini magneto-optical trap: A candidate for compact CPT cold atom-clocks

B.M. Xu^{a,b,c}, X. Chen^{a,b,c}, J. Wang^{a,b,*}, M.S. Zhan^{a,b}

^aState Key Laboratory of Magnetic Resonance and Atomic and Molecular Physics, Wuhan Institute of Physics and Mathematics, Chinese Academy of Sciences, Wuhan 430071, China

^bCenter for Cold Atom Physics, Chinese Academy of Sciences, Wuhan 430071, China

^cGraduate School, Chinese Academy of Sciences, Beijing 100080, China

ARTICLE INFO

Article history:

Received 26 May 2008

Received in revised form 7 August 2008

Accepted 9 August 2008

PACS:

32.80.-t

32.80.Pj

42.50.-p

ABSTRACT

We have demonstrated the experimental realization of a single-beam mini magneto-optical trap (MOT) of ⁸⁷Rb atoms, originally designed for a cold atom clock with coherent population trapping (CPT). Only one beam is used as cooling, trapping and repumping beams rather than the three pairs of orthogonal beams of the standard magneto-optical trap. The core optics, which consists of a modified pyramidal funnel type mirror, a quarter-wave plate and a retroreflect mirror, is installed inside a mini titanium cubic chamber. The vacuum system, rubidium source, magnetic field coils and beam expander are designed in a compact geometry. As many as 1.1×10^7 rubidium atoms are cooled and trapped, and thus the mini trap is ready for the implementation of a novel compact coherent population trapping cold atom-clock.

© 2008 Elsevier B.V. All rights reserved.

1. Introduction

Recently, a new type of atomic clock based on coherent population trapping (CPT) [1,2] has attracted more attention. It is different from traditional atomic clock approaches, such as atomic beam, atom fountains and optical pumped atom-clocks, CPT atom-clocks have no resonant absorption and thus greatly minimize the light shift. There are two main approaches for CPT atom clocks. One is a vapor cell passive atom-clock [3,4] in which the resonant signal based on the CPT phenomenon is detected directly via the radiation transmitted from the atomic vapor cell. The other is an active atomic clock [5] in which the resonance signal is obtained by stimulated emission in a microwave cavity-cell configuration. This active clock is also called a CPT-maser. The most significant advantage of the CPT clock is its potential for miniaturization and wide application. In this respect, the vapor cell passive atomic clock is more promising to integrate as a miniature device. For example, if one ignores stability, a passive CPT atomic clock can be realized on a chip scale size [6]. However, in most cases, we expect not only the compact size of a CPT clock, but also its excellent stability performance. A vapor cell passive clock uses hot atomic gas (the typical temperature is around 340 K) as the CPT medium, the linewidth of the resonance line being broadened by the Doppler effect, and thus the stability of

the clock is limited by the higher temperature of the vapor cell. An ideal scheme to improve the stability of the CPT clock is to use cold atoms instead of hot atomic vapor. Because of the lower velocity and the narrow velocity distribution of cold atoms, the Doppler broadening of the resonance line will be greatly minimized; this is useful for precise measurement of the atomic spectrum. In addition, cold atoms are more suitable for CPT because of their longer coherent time. Thus, a CPT clock based on a cold atom medium will display better precision and stability than a hot atomic vapor CPT clock. The main problem for a cold atom CPT clock is how to realize a miniature system. This is now possible due to the achievement of laser cooling and trapping techniques for neutral atoms.

Since the experimental realization of the magneto-optical trap (MOT) [7–9] in the middle of 1980s, there have been many steady improvements in trapping techniques for neutral atoms [10]. In a standard MOT, there are three pairs of orthogonal beams and a quadrupole magnetic field, while each pair of laser beams has opposite circular polarization σ^+ and σ^- . The quadrupole magnetic field is supplied by an anti-Helmholtz coil pair which carries appropriate current, the value of magnetic field depending on the special position and the position of minimum magnetic field being consistent with the intersection of three pairs of laser beams. Apart from the typical six-beam MOTs demonstrated by Chu et al. [9], Shimizu et al. realized a four-beam atom trap [11], consisting of a quadrupole magnetic field and four laser beams in a tetrahedral configuration, while a five-beam MOT configuration was demonstrated in 1999 [12]. The multi-beam MOTs require more optics and more complex experimental equipment, and are not suitable

* Corresponding author. Address: State Key Laboratory of Magnetic Resonance and Atomic and Molecular Physics, Wuhan Institute of Physics and Mathematics, Chinese Academy of Sciences, Wuhan 430071, China. Tel.: +86 27 8719 7375; fax: +86 27 8719 8576.

E-mail address: wangjin@wipm.ac.cn (J. Wang).

for a situation which needs a compact and simple MOT configuration, such as the CPT cold atom clock.

One of the simple MOT types is the single-beam atom trap, which can be used to satisfy the compact requirements of the CPT clock. The single-beam atom trap is based on a pyramidal or conical mirror [13,14], it can be modified as an axicon (conical hollow) mirror [15] used for cold atomic beam [16–20], atom optics [21], atom chips [22] and atomic guiding [23]. The size and geometry of this kind of trap depends on its purpose. For cold atomic beam, atom optics and atom guiding apparatus, in order to obtain a higher intensity of atom flux, giant-size mirror and laser beams are needed and thus it is not possible to shrink the trap system. On the other hand, just for trapping few atoms in atom chips, small size mirror and laser beams are sufficient. However, a cold atom CPT clock needs both a higher number density of atoms and a smaller trap size, it is necessary to re-design the single-beam MOT to maintain the balance between atomic number and trap size. To our knowledge, no one has reported a mini single-beam atomic trap for CPT clocks. Here, we demonstrate such a single-beam mini MOT which is suitable for compact CPT clocks.

2. Single-beam mini trap

The trap is made up of a modified pyramidal funnel type mirror, a quarter-wave plate and a retroreflecting mirror, the vacuum system, rubidium source, magnetic field coils and beam expander are designed in a compact geometry. As shown in Fig. 1, linearly polarized cooling (trapping) and repumping beams supplied by two diode lasers are combined together via a polarization beam splitter cube (PBS), and then coupled into a single-mode polarization maintaining fiber (SPMF); the spacial distribution of the laser beams is modified as perfect Gauss modes by the fiber. A coupling lens connected to the end of the fiber is used to obtain a 2 mm diameter collimated beam. To build a single-beam trap, a bigger diameter collimated beam is necessary. We designed and realized a telescope optical system with three lenses (L1, L2, and L3) for expanding and collimating the input slim laser beam, and obtained a wide beam with diameter of 35 mm. The expanded trapping and

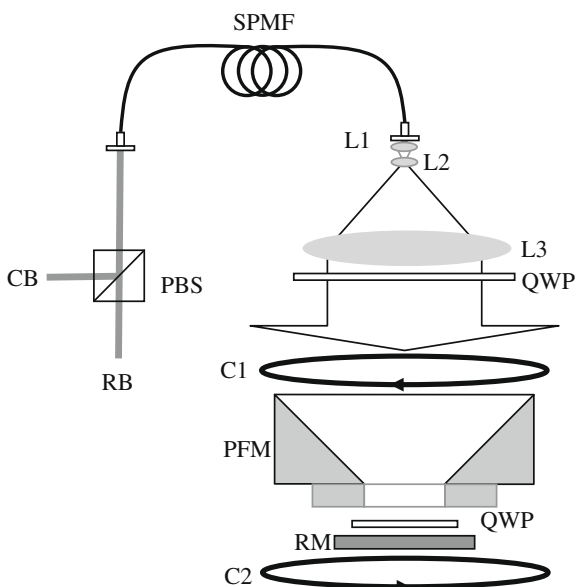


Fig. 1. Schematic diagram of the experimental setup, CB: cooling beam; RB: repumping beam; PBS: polarizing beam splitter; SPMF: single-mode polarization maintaining fiber; L1–L3: lens; QWP: quarter-wave plate; C1 and C2: coils; PFM: pyramidal funnel mirror; RM: retroreflecting mirror.

repumping beams are changed from linear polarization to circular polarization via a quarter-wave plate (QWP), and then irradiated on a modified pyramidal funnel type mirror (PFM) which is mounted in the middle of a titanium cube vacuum chamber; another QWP and a high reflectivity mirror are mounted under the PFM. The reason for choosing titanium is its lower remanence. An anti-Helmholtz coil pair (C1, C2) is mounted around the vacuum cube; the axes and the center point of the coils are coincident with the axes of the laser beams and the center of the PFM respectively.

The detailed design of the single-beam trap is described in Fig. 2. The PFM assembly is combined with mounting structure and glass mirrors, its longitudinal cross section (z - x plane) and 3-D view are shown in Fig. 2a and b. The mirror mount is made of an aluminum cylinder, the outside diameter of the cylinder top is 35 mm while the bottom is 20 mm, and this shrinker base is convenient for mounting. There is a pyramidal hollow in the top side of the cylinder, and each side cross section of the hollow pyramid has an obliquity of 45° . A square hole with 8 mm side in the bottom of the cylinder connects with the pyramidal hollow. Four fan-shaped dielectric mirrors are installed on four sectors of the pyramid using a special kind of high vacuum glue (ERO-TEK 353ND). With another QWP and a high reflectivity mirror, this setup can automatically produce three sets of counterpropagating beams if the incident laser beam is circular polarized as discussed in Ref [13]. For a σ^- polarized wide incident beam, each reflection from the two sides of the mirror generates two counterpropagating transverse beams with opposite polarizations, while the central part of the laser beam passes through the square hole, quarter-wave plate, then is reflected by the bottom mirror, and generates counterpropagating vertical beams with opposite polarizations. For the convenience of future CPT, a rectangular slot is notched along the diagonal of the x - y plane, so that laser beams for CPT pass through the slot and interact with the cold atom cloud. In addition, a rectangular slot enables fine adjustment of the CPT beams and the optimization of the overlap between the laser beam and the atoms.

The titanium cube is a critical part of the mini trap; in order to reduce the system as much as possible, we using a small cube chamber with a length of 70 mm. There are four viewports (CF-35) and two flanges (CF-16) on the chamber. The top anti-reflecting coated viewport is the entrance for the wide trap beam, the bottom high reflecting coated viewport is the retroreflecting mirror for the center square beam. The front and rear anti-reflecting coated

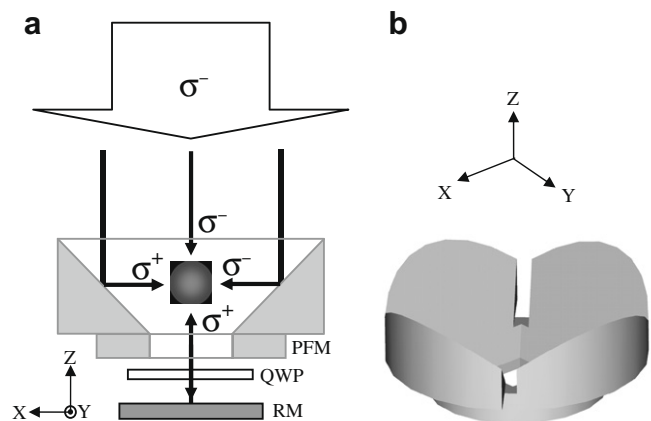


Fig. 2. Detailed design of single-beam trap, (a) is the longitudinal cross section of the single-beam optical configuration; (b) is the 3-D view of the pyramidal funnel mirror assembly, the rectangular slot along the diagonal of x - y plane is the route prearranged for CPT beams.

viewports are for transmitting the CPT light. All of four viewports are sealed to the cube chamber using indium thread. The right side flange is connected to a mini ion pump (Varian, 2 l/s), and the left side flange is connected to a rubidium dispenser and a right-angle metal valve via a Tee-type tube. The whole PFM assembly and QWP are mounted inside the cube chamber. The ion pump maintains the vacuum, and the metal valve is for connecting to a prepump at the initial stages of pumping. The dispenser is used as a mini atom source. When one applies DC current to a rubidium dispenser, it will heat up and release enough rubidium vapors into the vacuum chamber.

The telescope system for expanding and collimating the trapping beam includes three lenses L1, L2, and L3, all of the lenses are made of K9 glass and are anti-reflecting coated on both sides. In order to reduce the length of the system, two input lenses L1 and L2 are designed as concave lenses, while the output lens L3 is a double convex lens. The outside diameters of L1, L2 and L3 are 10 mm, 16 mm and 44 mm, respectively, the space between L1 and L2 is 38 mm, and the space between L2 and L3 is 40 mm. The curvatures of these lenses are well designed for perfect beam expanding and collimating. Three lenses are installed inside an aluminum cylindrical adjustable mount with a FC fiber connector on the input side and a QWP mount on the output side. We successfully obtained a wide circularly polarized Gaussian beam with a diameter of 35 mm from this telescope system. The profile of the output laser beam is checked by using a pinhole, a precision multi-axis positioning stage (Newport 562) and a power meter (Newport 1815-C-CAL). The experimental results of the output beam intensity along a diameter of the cross section are shown in Fig. 3. The dots are the experimental data, and the dashed curve is a Gaussian fit. It is obvious that the wide Gaussian beam obtained from this telescope system is ideal for our mini trap.

The quadrupole magnetic field for the mini trap is supplied by an anti-Helmholtz coil pair (C1 and C2), each coil is a 250-turn solenoid with an average diameter of 56 mm, and the space between two coils is 132 mm. To eliminate vertical geomagnetism and adjust the position of the minimum field, DC currents to C1 and C2 are controlled independently. To eliminate the horizontal remanence of the mini ion pump, a bias coil is placed near the left flange of the cube. Thus it is easy to change the center of the quadrupole magnetic field by adjusting the DC currents to C1, C2 and bias coil.

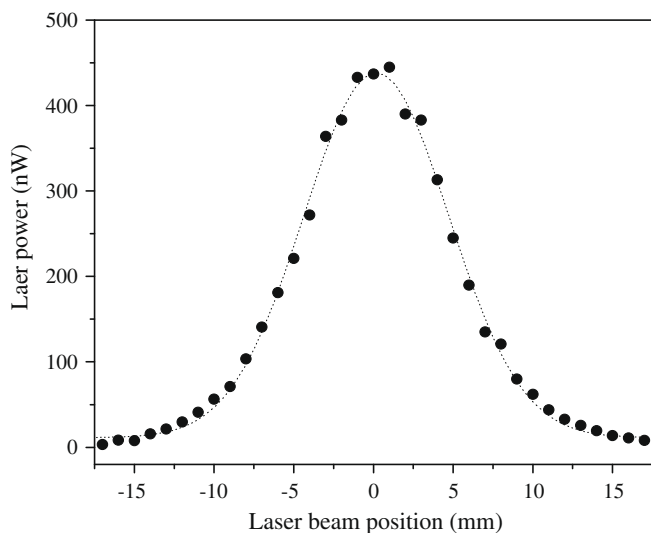


Fig. 3. Intensity distribution of the expanded and collimated laser beam, the dots are the experimental data recorded along the diametrical line of the cross section of the laser beam, and the dashed curves are Gaussian fits.

The laser which supplies the repumping beam (RB) is a commercial narrow linewidth diode laser (New Focus 6103) with center wavelength of 780 nm and output power of 15 mW. The laser which supplies the cooling beam (CB) is a homemade grating-stabilized external cavity diode laser, with a wavelength of 780 nm and an output power of 50 mW. The linewidth of the free-running laser is more than 10 MHz. A polarization spectroscopy method [24] is used to stabilize the frequency of the cooling laser, and its linewidth can be greatly reduced to less than 300 KHz.

3. Experimental results

The experiment is carried out by the following procedures. First, the whole vacuum system is thoroughly baked and pumped with a rotary vacuum pump and a turbo molecular pump, and then the mini ion pump is operated to maintain a high vacuum. The balanced vacuum pressure inside the cube chamber is 1.3×10^{-6} Pa, which is good enough for laser cooling and trapping of neutral atoms. Second, the laser, fiber and optical system are adjusted. The cooling laser frequency is tuned to the transition of ^{87}Rb : $5S_{1/2}(F=2) \rightarrow 5P_{3/2}(F=3)$ with a red-shift of 14 MHz, and narrowed by polarization spectroscopy. A 40 dB optical isolator is placed between the laser and the optics. About 40 mW laser beam is coupled into the fiber, and more than 20 mW laser beam is obtained from the telescope which is connected to the output side of fiber. The repumping laser beam is combined with the cooling beam via a PBS, and then coupled into the same fiber. An output power of 2.5 mW for the repumping beam is achieved behind the telescope system. The frequency of the repumping beam is tuned to the resonance of ^{87}Rb : $5S_{1/2}(F=1) \rightarrow 5P_{3/2}(F=2)$. Thirdly, the anti-Helmholtz coil pair and the bias coil are mounted as described above. DC currents with values of 3.0 A and 3.2 A are applied to the lower coil (C2) and upper coil (C1), respectively; an adjustable current supply is connected to the bias coil for optimizing the horizontal magnetic field. Under the above conditions, a quadrupole magnetic field with a central gradient of 9.0 Gauss/cm is formed. A 4.2 A DC current is applied to the rubidium dispenser via a feed-through flange, and rubidium vapor is released into the MOT region. To monitor the trap signal, a CCD camera is installed near the front viewport of the cube chamber, and the real-time video signal is sent to computer. Finally, the atoms are cooled and trapped in the mini MOT and a near-spherical bright cloud appears in the center point of the pyramidal funnel, as shown in Fig. 4. In contrast with the scattered light in the background, the brightness of the atom cloud is very sensitive to the laser frequency detuning and magnetic field.

The number of cold atoms trapped in the mini trap is measured using the calibrated sensitive power meter mentioned above. The loading time of this single-beam mini trap is 50 ms, and its life time is 5 ms. Atom numbers are dependent on laser intensity, laser detuning ($\sigma_{\text{laser}} - \sigma_{\text{atom}}$), and magnetic gradient. More atoms are trapped with higher intensities of cooling and repumping lasers. The dependence of cold atom numbers on the detuning of the cooling laser is shown in Fig. 5. Atom number changes with frequency detuning of the cooling laser; no atoms are trapped if the cooling laser frequency is exactly resonant with the atomic transition of ^{87}Rb : $5S_{1/2}(F=2) \rightarrow 5P_{3/2}(F=3)$, while under the optimal detuning value of -13.7 MHz, the maximum atom number of $(11.0 \pm 0.5) \times 10^6$ are achieved, but the number of cold atoms decreases when the laser detuning is less than -13.7 MHz.

For CPT test purposes, we investigated and obtained the absorption spectrum of these cold ^{87}Rb atoms by recording the transmitted signal of a probe laser beam. This probe beam is supplied by the third diode laser which is similar to the repumping laser (New Focus 6103), and the laser frequency is scanned across the transition

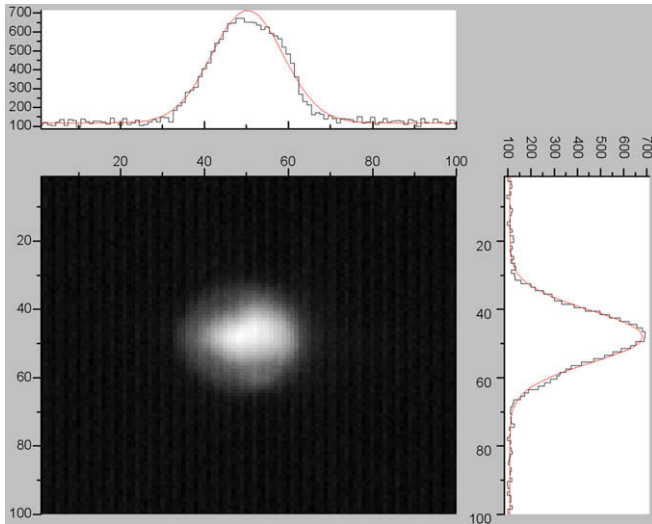


Fig. 4. Image of the mini MOT recorded by a CCD camera and displayed on computer interface. The near-spherical bright cloud located in the center is due to the cold ^{87}Rb atoms trapped in the mini MOT. A horizontal and vertical intensity profile is also displayed on the top and right side, respectively.

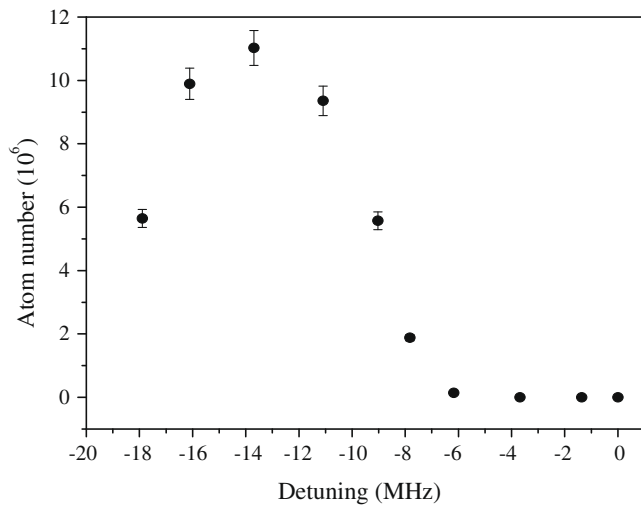


Fig. 5. Dependence of cold atom numbers on the detuning of the cooling laser. No atoms are trapped if the cooling laser frequency is exactly resonant with atomic transition of ^{87}Rb : $5S_{1/2}(F=2) \rightarrow 5P_{3/2}(F=3)$, while atom number increases with frequency detuning of laser, and the optimal detuning value is -13.7 MHz which corresponds to the maximum atom number of $(11.0 \pm 0.5) \times 10^6$, and a further increase in the absolute detuning value causes the reduction of cold atom numbers in the trap.

of ^{87}Rb : $5S_{1/2}(F=2) \rightarrow 5P_{3/2}(F=3)$. As shown in Fig. 6, both Doppler free absorption peaks of cold ^{87}Rb atoms (a) and Doppler broadened absorption profile of background hot ^{85}Rb atoms (b) appeared when the scanning span of probe laser is wider enough. It is obviously that the cold atoms have narrower absorption peak than hot atomic vapor, and that is the main reason we will select cold atoms for the CPT clock.

Fig. 6 shows that the measured absorption signal for the background hot atoms is fairly large; this is due to higher Rb vapor pressure (1.3×10^{-6} Pa) in the trap. Normally the trap works better with a smaller vapor pressure (for example, less than 2×10^{-7} Pa), under which the contribution to the absorption signal from the hot atoms is negligible. But in our experimental configuration, in order to realize a compact MOT, we adopted a mini ion pump (2 l/s), and the best pressure level of present setup is 10^{-6} Pa. If a better ion

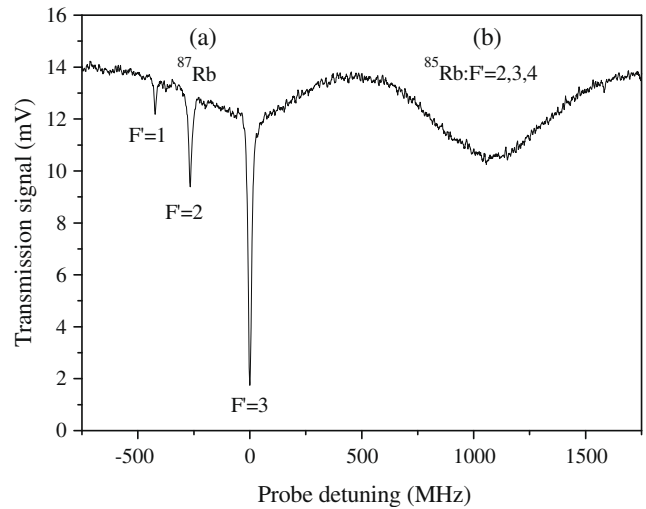


Fig. 6. Absorption spectra of rubidium atoms in the single-beam mini trap, (a) Doppler free absorption peak of cold ^{87}Rb atoms for ^{87}Rb : $5S_{1/2}(F=2) \rightarrow 5P_{3/2}(F=1, 2, 3)$; (b) Doppler broadened absorption profile of background hot ^{85}Rb atoms, corresponding to the transition ^{85}Rb : $5S_{1/2}(F=3) \rightarrow 5P_{3/2}(F=2, 3, 4)$.

pump is used or a better baking and pumping procedure is applied at the beginning of system preparation, the final vapor pressure should be lower than present value and the absorption signal should be cleaner. Any how, the present spectrum is good enough for CPT purposes.

4. Conclusion

In summary, we designed and realized a novel single-beam mini MOT. This trap is made up of a modified pyramidal funnel type mirror. The vacuum chamber, the rubidium source, the magnetic field coils and the beam expander are highly compact, and the geometry of the trap is suitable for mini-type cold atom clock. We successfully cooled and trapped more than 1.1×10^7 rubidium atoms in this trap, and obtained the absorption spectrum of these cold atoms. Further improvement towards the realization of a compact CPT cold atom clock will be carried out in the near future.

Acknowledgements

This research has been supported by the National Basic Research Program of China under Grant Nos. 2005CB724505/1 and by the National Natural Science Foundation of China under Grant No. 10774160. We thank Zhao for his technical support.

References

- [1] H.R. Gray, R.M. Whitley, C.R. Stroud, *Opt. Lett.* 3 (1978) 218.
- [2] J. Vanier, *Appl. Phys. B* 81 (2005) 421.
- [3] M. Merimaa, T. Lindvall, I. Titttonen, E. Ikonen, *J. Opt. Soc. Am. B* 20 (2003) 273.
- [4] L. Liu, T. Guo, K. Deng, X.Y. Liu, X.Z. Chen, Z. Wang, *Chin. Phys. Lett.* 24 (2007) 1883.
- [5] A. Godone, F. Levi, S. Micalizio, C. Calosso, *Phys. Rev. A* 70 (2004) 012508.
- [6] S. Knappe, V. Shah, P.D.D. Schwindt, L. Hollberg, J. Kitching, L.-A. Liew, J. Moreland, *Appl. Phys. Lett.* 85 (2004) 1460.
- [7] S. Chu, L. Hollberg, J.E. Bjorkholm, A. Cable, A. Ashkin, *Phys. Rev. Lett.* 55 (1985) 48.
- [8] W.D. Phillips, J.V. Prodan, H.J. Metcalf, *J. Opt. Soc. Am. B* 2 (1985) 1751.
- [9] S. Chu, J.E. Bjorkholm, A. Ashkin, A. Cable, *Phys. Rev. Lett.* 57 (1986) 314.
- [10] W.D. Phillips, *Rev. Mod. Phys.* 70 (1998) 721.
- [11] F. Shimizu, K. Shimizu, H. Takuma, *Opt. Lett.* 16 (1991) 339.
- [12] A. di Stefano, D. Wilkowski, J.H. Muller, E. Arimondo, *Appl. Phys. B* 69 (1999) 263.
- [13] K.I. Lee, J.A. Kim, H.R. Noh, W. Jhe, *Opt. Lett.* 21 (1996) 1177.
- [14] A.S. Mellish, A.C. Wilson, *Am. J. Phys.* 70 (2002) 965.
- [15] J.A. Kim, K.I. Lee, H.R. Noh, W. Jhe, M. Ohtsu, *Opt. Lett.* 22 (1997) 117.

- [16] A. Camposeo, A. Piombini, F. Cervelli, F. Tantussi, F. Fuso, E. Arimondo, *Opt. Commun.* 200 (2001) 231.
- [17] J.M. Kohel, J. Ramirez-Serrano, R.J. Thompson, L. Maleki, J.L. Bliss, K.G. Libbrecht, *J. Opt. Soc. Am. B* 20 (2003) 1161.
- [18] N. Lundblad, D.C. Aveline, R.J. Thompson, J.M. Kohel, J. Ramirez-Serrano, W.M. Klipstein, D.G. Enzer, N. Yu, L. Maleki, *J. Opt. Soc. Am. B* 21 (2004) 3.
- [19] S. Chaudhuri, S. Roy, C.S. Unnikrishnan, *Phys. Rev. A* 74 (2006) 023406.
- [20] N. Castagna, J. Gúena, M.D. Plimmer, P. Thomann, *Eur. Phys. J. Appl. Phys.* 34 (2006) 21.
- [21] H.R. Noh, W. Jhe, *Phys. Rep.* 372 (2002) 269.
- [22] M. Trupke, F. Ramirez-Martinez, E.A. Curtis, J.P. Ashmore, S. Eriksson, E.A. Hinds, Z. Moktadir, C. Gollasch, M. Kraft, G.V. Prakash, J.J. Baumberg, *Appl. Phys. Lett.* 88 (2006) 071116.
- [23] E. Dimova, O. Morizot, G. Stern, C.L. Garrido Alzar, A. Fioretti, V. Lorent, D. Comparat, H. Perrin, P. Pillet, *Eur. Phys. J. D42* (2007) 299.
- [24] C.P. Pearman, C.S. Adams, S.G. Cox, P.F. Griffin, D.A. Smith, I.G. Hughes, *J. Phys. B* 35 (2002) 5141.